The structural and spectroscopic properties for uranium oxides

Li Peng(李 鹏)[a], Jia Ting-Ting(贾婷婷)[a], Gao Tao(高 涛)[a]†, and Li Gan(李 赣)[b]

[a] *Institute of Atomic and Molecular Physics, Sichuan University, Chengdu* 610065, *China*
[b] *National Key Laboratory for Surface Physics and Chemistry, Mianyang* 621907, *China*

(Received 10 May 2011; revised manuscript received 1 July 2011)

The equilibrium structures, the charge population, and the spectroscopic properties of UO, UO_2, UO_3, and U_2O_3 molecules are systematically investigated using the density functional theory (DFT) with the method of generalized gradient approximation (GGA). The bond lengths and the vibrational frequencies of the ground states of UO, UO_2, and UO_3 molecules are all in agreement with available experimental data. For U_2O_3 molecules, our calculations indicate that the ground state of the U_2O_3 molecule is an $\tilde{X}^7A_1'$ state with D_{3h} (trigonal bipyramid) symmetry (R_1(U–O)=0.2113 nm, R_2(U_1–U_2)=0.2921 nm, $\angle U_1OU_2 = 87.5°$, dihedral angle Θ(U,O_1,O_2,O_3)=62.40°). The harmonic frequency, the IR intensity and the spin density of the U_2O_3 molecule are all obtained for the first time in theory. For the ground state of U_2O_3 molecules, the vibrational frequencies are 178.46 (A_1'), 276.79 (E_1''), 310.77 (E_1'), 396.63 (A_2''), 579.15 (E_1'), and 614.98 (A_1') cm^{-1}. The vibrational modes corresponding to the IR maximum peaks are worked out for UO_3 and U_2O_3 molecules. Besides, the results of Gophinatan–Jug bond order indicate that UO, UO_2, and UO_3 molecules possess U=O double bonds and that the U_2O_3 molecule possesses U–O single bonds and a U–U single bond.

Keywords: uranium oxides molecule, molecular geometry, charge population, vibrational spectrum

PACS: 33.20.–t, 31.15.ae, 31.15.A– **DOI:** 10.1088/1674-1056/21/4/043301

1. Introduction

The physical and the chemical properties of the actinide elements are an important research area for rational handling of nuclear materials.[1] Uranium, one of the important late actinide elements, has drawn much attention for its nuclear property and wide application in energy generation. Uranium is a highly reactive metal and it reacts with almost all of the nonmetallic elements and many of their compounds. The metal tarnishes in air, resulting in a dark layer of oxide. When finely powdered, uranium ignites spontaneously in air. The existence of unusual uranium oxide gaseous species of high stability in addition to the known UO(g), UO_2(g), and UO_3(g) molecules may be of importance in pressure-volume-temperature (PVT) data assessment for uranium oxygen systems at very high temperatures.[2] In the course of multipurpose mass spectrometric studies on high temperature vaporization of (Eu_2O_3 + UO_2 + WO_3) and of ($EuPO_4$ + UO_2) powders, Guido and Balducci[2] found the U_2O_3(g) species for the first time. Hence, the complete uranium oxides molecular structure and spectral data are essential to study the secure storage of the uranium.

Quantum chemistry calculations are now reaching a level of sophistication where they may provide accurate results for lanthanide and actinide compounds. These advances offer the possibility that actinide chemistry may soon be explored by computational methods, thereby circumventing many hazardous and expensive experimental studies.[3] However, the study of uranium molecules presents a challenge for experimental and theoretical researchers. The nearly degenerate 5f, 6d, 7s, and 7p orbitals give rise to a multitude of possible configuration interactions and a large number of electrons, open f and d shells, and strong relativistic effects must be taken into account.[4,5] For uranium oxides, in Refs. [6]–[9] the UO, UO_2, and UO_3 molecules trapped in rare gas matrixes were investigated. In 2000, Gagliardi and Roos[10] studied the uranium triatomic compounds XUY (X, Y=C, N, O) using the multiconfigurational second-order perturbation theory (CASSCF/CASPT2) and the density functional theory (DFT). In 2001, Gagliardi *et al.*[11] further calculated the electronic structure of the UO_2 molecule. They found UO_2 has a $^3\Phi_u$ ground state. In 2003, Christopher Lue *et al.*[3] measured the electronic spectrum of UO_2 isolated in a solid Ar matrix. In 2005, Gagliardi *et al.*[5] continued to study the elec-

†Corresponding author. E-mail: gaotao@scu.edu.cn

© 2012 Chinese Physical Society and IOP Publishing Ltd

tronic spectrum of the UO_2 molecule using spin–orbit coupling, and they confirmed that the ground state of UO_2 is $\tilde{X}^3\Phi_u$ ($\Omega = 2$). UO_3 was studied at the SCF level by Pyykkö *et al.*[12] who described a planar, almost T-shaped species with C_{2v} symmetry. Studies by Zhou *et al.*[6] indicated that the ground state of the UO_3 molecule is $\tilde{X}^1A_1$.

The structures, the properties, and the chemical bonds of the actinides oxides have been the focus of numerous theoretical and experimental studies due to the actinides element f orbital. We present a theoretical study on UO, UO_2, UO_3, and U_2O_3 molecules. We focus our attention on four aspects: (i) to find out the ground state structure of the U_2O_3 molecule; (ii) to ascertain the chemical stability of the U_2O_3 molecule; (iii) to analyse the population properties and bond orders of the UO_3 and U_2O_3 molecules; (iv) to acquire the infrared spectral data of the UO_3 and U_2O_3 molecules. The computational methods are described in Section 2. The calculated results are presented in Section 3, including four parts concerning geometries, electronic properties, population properties, and bond orders, and spectrum analysis, followed by a conclusion in Section 4.

2. Computational method

All calculations were performed with the density functional theory implemented in the ADF package.[13–21] Lyon *et al.*[22] used the ADF to study the formation of unprecedented actinide≡carbon triple bonds. Zhang and Li[23] used the ADF to study the molecular structures and the vibrational frequencies of uranium hexahalides UX_6 (X=F, Cl, Br, and I). Their study results are in good agreement with the recent experimental data. In the method, the DFT has been used successfully to study the physical and the chemical properties of uranium and plutonium systems.[22,24–26] We used the spin-polarized generalized gradient approximation (GGA) with OPTX exchange with PBE correlation (OPBE) functional for the exchange and correlation (XC) interaction, and double zeta no polarized basis sets (DZ). The scalar relativistic (SR) zero order regular approximation (ZORA)[27,28] was adopted to account for relativistic effects. Self-consistent field calculations were done with a convergence criterion of 10^{-6} Hartree (1 Hartree=27.21 eV) on the total bonding energy. A 0.001 Hartree electron smearing was applied to the molecular orbital occupation. In the geometry optimization, the converge thresholds were set to be 10^{-3} Hartree for the energy, 10^{-2} Hartree/Å (1 Å=0.1 nm) for the gradient and 10^{-2} Å for the radial. We started with the lowest spin multiplicity for the UO, UO_2, UO_3, and U_2O_3 molecules, then performed the spin-unrestricted calculations for all possible spin multiplicities. In as much as the 6s and 6p orbitals are important for uranium bonding, they are included explicitly in the variational space along with the 5f, 6d, and 7s valence orbitals, therefore, medium frozen-core approximation was applied to the U [$1s^2$-$5d^{10}$] atomic core. For oxygen atoms, we included 6 electrons from 2s and 2p orbitals.

3. Results and discussion

3.1. Equilibrium structure

For UO and $UO_2(D_{\infty h})$, we considered the possible multiplicity and proceeded geometry optimization. The ground state of the U atom is $^5L_6$ and that of the O atom is $^3P_2$. The possible multiplicities, the total bonding energies and the bond lengths are listed, in Table 1.

Table 1. Equilibrium structures for UO and UO_2 ($D_{\infty h}$) molecules.

UO				UO_2 ($D_{\infty h}$)			
Multiplicity[a]	E/eV[b]	R/nm	Exp[29]/nm	Multiplicity[a]	E/eV[b]	R/nm	Exp[6]/nm
3	–13.0271	0.1848		1	–19.7941	0.1839	
5	–13.4105	0.1856	0.1838	3	–23.2782	0.1823	0.1800
7	–5.0988	0.2203		5	–20.8348	0.1901	

[a] Multiplicity(Multi). [b] Total bonding energies (E).

As shown in Table 1, the ground state of UO is a quintet state. For UO_2, the triplet state has the lowest energy, and its electronic state is $\tilde{X}^3\Phi_u$. The U–O distances in UO and UO_2 molecule equilibrium structures are 0.1856 nm and 0.1823 nm, respectively, which are in agreement with the experimental values of 0.1838 nm and 0.1800 nm. So the method of the GGA/OPBE should be feasible to extend to the com-

putation of uranium oxides molecules.

The accurate electronic state for the ground state is of importance to study molecular properties. As a significant uranium compound, the electronic state of UO_2 has been the subject of several recent theoretical and experimental studies, owing to the fact that the guest–host interaction in rare gas matrixes will change the ordering of the states.[4,5,30] An intriguing feature was found in our process of geometric optimization for the UO_2 molecule, which is the electronic state changing between $^3\Phi_u$ and $^3\Delta_u$. In order to determine which electronic state corresponds to the ground state, we have specified occupation numbers to the gate geometric structure and performed re-optimization. The calculations indicate that in comparison with total bonding energy of $^3\Delta_u$ (−23.1438 eV), the total bonding energy of $^3\Phi_u$ state is low (−23.2292 eV), the energy gap between the two states is 0.0854 eV, which is in qualitative agreement with the previous theoretical result of Gagliardi *et al.*[5] Gagliardi *et al.* indicated that the energy gap between $^3\Phi_u$ and $^3\Delta_u$ is 1990 cm^{-1} (0.2467 eV), and pointed out that these two states are in spin–orbit free and $^3\Phi_u$ and $^3\Delta_u$ have the same electronic configuration (5f) (7s). Using spin–orbit coupling, they confirmed that the ground state of UO_2 is $\tilde{X}^3\Phi_u$ ($\Omega = 2$). The spin contamination of our calculation was checked to prove the credibility of the data, the S^2 expectation value ($\langle S^2 \rangle$) is 2.0097, for triplet state ($s = 1$) the exact value of S^2 is 2; the difference of two values is 0.0097, which demonstrates that the spin contamination for this molecular structure is very small.

For the UO_3 molecule, the most possible molecular structures are C_{2v}, D_{3h}, and C_{3v}. The depicted structures are presented in Fig. 1. Using the same method as that mentioned above, the possible multiplicity, the total bonding energies, and the bond lengths of the UO_3 molecule have been calculated, the results are listed in Table 2.

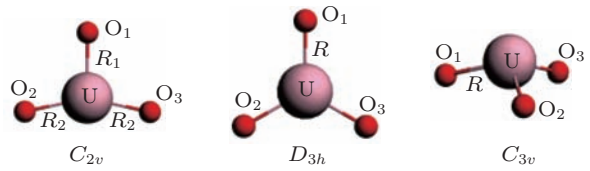


Fig. 1. (colour online) Geometries of UO_3 molecule.

Table 2. Ground state equilibrium structure for UO_3 molecule.

	Multiplicity[a]	E/eV[b]	R_1/nm[c]	R_2/nm[d]	Angle/(°)[e]
C_{2v}	1	–32.398	0.1870	0.1841	154.7
	3	–30.616	0.1904	0.1854	162.0
	5	–27.605	0.1928	0.1928	119.7
	7	–23.485	0.2198	0.1986	173.3
	Ref. [6]	–	0.1853	0.1810	158.8

[a] Multiplicity (Multi). [b] Total bonding energies (E). [c] The distance of U–O_1. [d] The distance of U–O_2 (O_3). [e] The angle of O_2–U–O_3.

The ground state equilibrium geometry of the UO_3 molecule is an almost T-shaped structure with C_{2v} symmetry. By comparison with the total bonding energies of different multiplicities, we find that the ground state of UO_3 is singlet. Its electronic state is $\tilde{X}^1A_1$. Our study shows that the D_{3h} geometry for UO_3 is not in a true minimal energy state; it has a doubly degenerate imaginary frequency that leads to the almost T-shaped minimal energy structure, which is in agreement with the previous theoretical result given by Zhou *et al.*[6] For C_{3v} geometry of UO_3, almost all the results tend to be of D_{3h} geometry, eventually it is converted into almost T-shaped minimal energy structure.

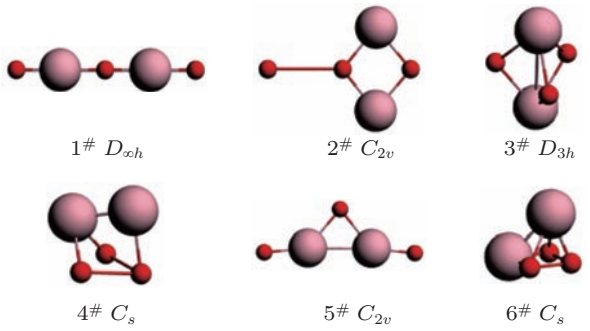


Fig. 2. (colour online) The most possible molecular structures of the U_2O_3 molecule.

The ground state equilibrium structure of the U_2O_3 molecule has been found to be of a trigonal bipyramid with D_{3h} symmetry. In the process of optimization, 15 kinds of possible structures have

been designed; the most possible molecular structures and their corresponding symmetries are presented in Fig. 2. The difference between $4^{\#}$ (C_s) and $6^{\#}$ (C_s) symmetries is that in $6^{\#}$ (C_s) structure, there is a uranium atom in the same plane as where the three oxygen atoms stay. Possible multiplicities, total bonding energies of molecular structures are listed, respectively, in Table 3. After optimizing these structures mentioned above, we find that most geometry structures are unstable, such as $6^{\#}$ (C_s) geometry; the uranium atom which is in the plane where the three oxygen atoms stay moves to another vertex of the trigonal bipyramid and eventually it is converted into an equilibrium structure. From Table 3, we can see the total bonding energy of the septet state is lowest. The corresponding bond length, angles, and dihedral angle are listed in Table 4.

Table 3. Total bonding energies of different multiplicities.[a]

Multiplicity[b]	$1^{\#}$	$2^{\#}$	$3^{\#}$	$4^{\#}$	$5^{\#}$	$6^{\#}$
3	–38.1048	–	–39.5288	–40.0305	–	–
5	–38.3303	–31.8849	–40.2909	–	–40.3132	–
7	–39.1224	–32.3529	–40.4617	–	–40.1920	–
9	–32.2334	–31.7559	–36.8287	–	–36.9109	–
11	–31.1695	–32.1265	–32.2589	–	–	–
13	–26.8644	–28.5845	–28.9609	–24.4902	–	–

[a]The unit of energy is eV. [b]Multiplicity (Multi). – Convergence failure.

Table 4. Bond lengths and angles for the ground state of the U_2O_3 molecule (D_{3h}).

Bond length/nm			Angle/(°)		
R_1	R(U[a], Ox[b])	0.2113	A	A(U_1, Ox, U_2)	87.5
R_2	R(U_1, U_2)	0.2921	Θ	Θ(U,O_1,O_2,O_3)	62.40

[a]U_1 or U_2. [b]$x = 1, 2, 3$.

Using the theory of direct products of representation,[31] we determined the ground state of U_2O_3 with D_{3h} symmetry to be $\tilde{X}^7A_1'$. The corresponding energy of the highest occupied molecular orbital (HOMO) of α orbital is -1.9106 eV, the energy of the lowest unoccupied molecular orbital (LUMO) of α orbital is -2.0325 eV, the energy gap is 0.1165 eV; for β orbital, the energy of HOMO is -5.5155 eV, the energy of LUMO is -1.3179 eV, the energy gap is 4.1976 eV. As shown by the HOMO–LUMO gaps of probable structures for septet state listed in Table 5, the largest gap corresponds to D_{3h} structure, which indicates the U_2O_3 molecule with D_{3h} symmetry has higher chemical stability because it is energetically unfavourable for adding electrons to a high-lying LUMO or extracting electrons from a low-lying HOMO.[32] The orbital contributions to HOMO and LUMO in the ground state of the U_2O_3 molecule are listed in Table 6. The HOMO–LUMO of α orbital is contributed mainly by $5f$ orbital of a U atom, while the HOMO of β orbital is contributed mainly by 2p orbital of an O atom and the LUMO (β) is contributed mainly by 7s orbital of a U atom. Hence, in electrophilic attack, the reagent will selectively attack the 5f orbital of the U atom and 2p orbital of the O atom; 7s orbital of the U atom will be the most vulnerable to the attack by nucleophile. Besides, the S^2 expectation value ($\langle S^2 \rangle$) is 12.0376, and for septet state ($s = 3$) the exact value of S^2 is 12, so the difference between the two values is 0.0376.

Table 5. HOMO and LUMO gaps of probable structures for the septet state of U_2O_3.

Orbital	E/eV	$1^{\#}$ ($D_{\infty h}$)	$2^{\#}$ (C_{2v})	$3^{\#}$ (D_{3h})	$5^{\#}$ (C_{2v})
α	HOMO	–2.4236	–2.6051	–1.9160	–3.8864
	LUMO	–2.4781	–2.5939	–2.0325	–3.8086
	gap	0.0545	0.0112	0.1165	0.0778
β	HOMO	–5.5308	–4.1679	–5.5155	–6.9190
	LUMO	–2.2490	–2.3079	–1.3179	–3.3076
	gap	3.2818	1.8600	4.1976	3.6114

Table 6. HOMO and LUMO percentages (%) for the ground state of the U_2O_3 molecule (D_{3h}).

U_2O_3			U				O	
		MO	6p	5f	6d	7s	2s	2p
α	HOMO	$3e''_1$		88.13	11.48			
	LUMO	$1a''_1$		99.99				
β	HOMO	$1a'_2$		6.97				92.39
	LUMO	$5a'_1$	1.78	26.42	3.91	67.68	–1.38	1.94

3.2. Population properties

In order to further study the electronic structure of uranium oxide, we have discussed the charge population properties and the spin densities of the ground states for UO, UO_2, UO_3, and U_2O_3 molecules: the results are detailed in Table 7. The symbols (U_1, O_2, etc.) in the table are corresponding to those in Fig. 3. Because natural bonding orbital (NBO) analysis in an ADF package cannot handle frozen cores currently, we use the Mulliken populations to qualitatively describe charge population properties.

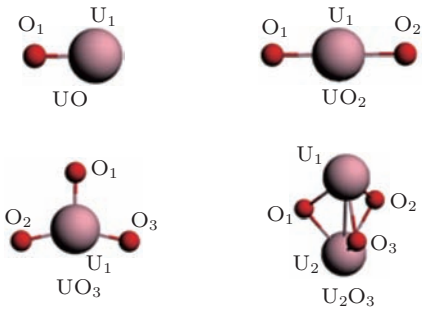


Fig. 3. (colour online) Equilibrium structures of UO, UO_2, UO_3, and U_2O_3 molecules.

Table 7. Population properties for UO, UO_2, UO_3, and U_2O_3 molecules.

Molecule	Atom	Charge	Spin density	Total
UO	U_1	0.5428	4.1842	[core] $5f^{3.499}6p^{5.955}6d^{1.110}$ $(6s+7s)^{2.889}$
	O_1	–0.5428	–0.1842	[core] $2s^{1.981}$ $2p^{4.553}$
UO_2	U_1	0.7966	2.1580	[core] $5f^{3.083}$ $6p^{5.887}6d^{1.398}$ $(6s+7s)^{2.834}$
	O_1	–0.3983	–0.0790	[core] $2s^{2.005}$ $2p^{4.394}$
	O_2	–0.3983	–0.0790	[core] $2s^{2.005}$ $2p^{4.394}$
UO_3	U_1	1.3616	0.0000	[core] $5f^{3.062}$ $6p^{5.861}6d^{1.717}$ $(6s+7s)^{1.999}$
	O_1	–0.4413	0.0000	[core] $2s^{2.011}$ $2p^{4.467}$
	O_2	–0.4413	0.0000	[core] $2s^{2.009}$ $2p^{4.432}$
	O_3	–0.4413	0.0000	[core] $2s^{2.009}$ $2p^{4.432}$
U_2O_3	U_1	1.1100	3.1805	[core] $5f^{3.345}$ $6p^{5.969}6d^{1.368}$ $(6s+7s)^{2.206}$
	U_2	1.1100	3.1805	[core] $5f^{3.345}$ $6p^{5.969}6d^{1.368}$ $(6s+7s)^{2.206}$
	O_1	–0.7400	–0.1203	[core] $2s^{1.996}$ $2p^{4.744}$
	O_2	–0.7400	–0.1203	[core] $2s^{1.996}$ $2p^{4.744}$
	O_3	–0.7400	–0.1203	[core] $2s^{1.996}$ $2p^{4.744}$

As seen from Table 7, in all the uranium oxides, the uranium atom always loses an electron, thereby becoming an electron donor and the oxygen atom always obtains an electron, thus becoming an electron acceptor. This characteristic can also be confirmed by the electronegativity. The electronegativity of the oxygen atom is 3.44, which is much larger than uranium atom electronegativity 1.70,[33] so the oxygen atom can easily obtain an electron from the uranium atom.

The charge population results indicate that there are hybrid orbitals mixing 5f, 6d, and 7s orbitals of uranium with the 2p orbital of oxygen in UO, UO_2, UO_3, and U_2O_3 molecules. In our calculations, we included 14 electrons from the 5f, 6s, 6p, 6d, and 7s orbitals of the uranium. As shown by the charge population results listed in Table 7, the electron number of 6s+7s orbitals of the uranium atom in uranium ox-

ide is less than that of the same orbitals of the neutral uranium atom which has 4 electrons. However, in neutral uranium atom, the energy of 6s orbital is −52 eV and 7s orbital is −6.1 eV,[33] which is much higher than that of 6s orbital. Therefore, the electrons of the 7s orbital should be easier to lose than those of the 6s orbital. The charge transfers from the uranium 7s orbital to the 5s, 6d, and oxygen 2p orbitals. This significant hybridization or orbital mixing between 5f, 6d, and 7s orbitals of uranium and the 2p orbital of oxygen also enhances the bonding strengths of the U–O bonds.

Through the analysis of the spin density, we found that the uranium atom makes positive contributions to the total spin multiplicities for UO, UO_2, and U_2O_3 molecules, while oxygen always contributes to negative spin. For the UO_3 molecule, the ground state is of holosymmetry, so the spin density of UO_3 ground state is zero. The value of total spin density is equal to the number of spin polarization (2s).

The molecular orbital (MO) percentage analysis of the ground state of U_2O_3 indicates that with orbital energy rising, the contributions of the 5f orbital of the U atom and the 2p orbital of the O atoms to MO increase, and the 5f orbital is dominant at higher energy orbit; while the 6p orbital of the U atom and the 2s orbital of the O atom contribution decrease, and the results are listed in Table 8.

Table 8. Molecular orbital (MO) percentages (%) of valence and semicore orbitals in U_2O_3 molecule.

U_2O_3	U					O	
MO(α)	6s	6p	5f	6d	7s	2s	2p
$1e'$		52.10				44.02	2.34
$1e''$		97.25					3.41
$2a_2''$		97.00					2.85
$2e_1'$		46.18		2.52		51.37	
$3a_1'$		35.76				64.57	
$3e_1'$		1.05	9.15	18.49		1.68	69.95
$2e_1''$		2.42	5.57	20.68			71.14
$4a_1'$		5.53	2.12	27.18	1.07		61.33
$3a_2''$		2.05	10.82		10.73		76.07
$4e_1'$			12.54	4.42		2.03	79.58
$1a_2'$			12.82				86.50
$5a_1'$			85.10		10.06		4.37
$6a_1'$			92.05		6.59		

The Gophinatan–Jug bond orders in uranium oxide molecules are quite different, and the results are listed in Table 9. The symbols (U_1, O_2, etc.) in the table are corresponding to those in Fig. 3. The U–O bond orders are 2.37, 2.41, 2.47, and 2.41 for UO, UO_2, and UO_3, respectively, showing that UO, UO_2, and UO_3 molecules all possess double bonds; for the U_2O_3 molecule, the U–O bond order indicates that it has single bond, an d U_1–U_2 bond order (1.60) reveals the single bond properties. However, the U_1–U_2 bond order in the U_2 molecule is 5.92 (with bond length 0.2407 nm and the same computation method as that shown in the context), which demonstrates that U and O are easier to bond than U and U in uranium oxides.

Table 9. Gophinatan–Jug bond orders in UO, UO_2, UO_3, U_2O_3, and U_2 molecules.

	U_1–O_1	U_1–O_2	U_1–O_3	U_2–O_1	U_2–O_2	U_2–O_3	U_1–U_2
UO	2.37						
UO_2	2.41	2.41					
UO_3	2.47	2.41	2.41				
U_2O_3	1.17	1.17	1.17	1.17	1.17	1.17	1.60
U_2							5.92

3.3. Spectrum analysis

The irreducible representations corresponding to the vibrations, the frequencies and the absorption intensities for the ground states of UO, UO_2, and UO_3 molecules are presented in Table 10. The vibrational frequencies and the absorption intensities for the different modes of the ground state of the U_2O_3 molecule are listed in Table 11. Besides, the vibrational spectra of the four lowest-energy structures are all shown in Fig. 4. Figure 5 i llustrates the vibrational modes for the ground state of the U_2O_3 molecule, in which the vibrational direction is shown with the black arrowhead. There are $3n-5$ vibrational degrees of freedom for a linear molecule, and $3n-6$ ones for a nonlinear molecule. Hence, the UO molecule has 1 vibrational degree of freedom; the UO_2 molecule has 4 vibrational degrees of freedom, two of them are degenerate vibration, 6 vibrational degrees of freedom for the UO_3 molecule, and 9 vibrational degrees of freedom for the U_2O_3 molecule.

Table 10. Vibrational modes (Mode), frequencies, and absorption intensities (IR. int) for the ground states of UO, UO_2, and UO_3 molecules.

Molecule	Mode	v (calc.)/cm^{-1}	Ref.[a]	v (exp.)/cm^{-1}[b]	IR. int/(km/mole)
UO	σ	869.12	846	889.5	200.745
UO_2	π_u	80.92	–	138	83.017
	σ_g	863.38	875	859	0.000
	σ_u	936.25	937	914.8	375.321
UO_3	a_1	130.21	262	186.2	39.114
	b_2	156.90	242	211.6	15.892
	b_1	163.87	214	151.5	50.646
	a_1	792.33	838	745.5	165.393
	a_1	865.73	964	–	31.965
	b_2	880.02	991	852.6	369.068

[a]UO data cited from Ref. [6] theoretical calculations, UO_2 from Ref. [11], UO_3 from Ref. [12]. [b]UO and UO_2 from Ref. [6] experimental results, UO_3 from Ref. [34].

Table 11. Vibrational frequencies for different modes of the ground state of U_2O_3 molecule.

Mode	Frequencies/cm^{-1}	IR. int/(km/mole)
a_1'	178.46	0.000004
e_1''	276.79	0.000000
e_1''	276.79	0.000000
e_1'	310.77	32.726167
e_1'	310.77	32.726167
a_2''	396.63	63.519435
e_1'	579.15	176.681036
e_1'	579.15	176.681036
a_1'	614.98	0.000001

The vibrational frequencies of isolated UO_2 have been computed. As shown in Table 10, our results reveal the antisymmetric stretch of UO_2 at 936.25 cm^{-1} and the symmetric stretch of UO_2 at 863.38 cm^{-1}. In recent years, vibrational frequency of UO_2 has received a great deal of attention, because the unusual behaviour of the matrix-isolated molecule is exhibited as the noble–gas host is changed.[30] The antisymmetric stretch of UO_2 was observed at 914.8 cm^{-1} in an Ne matrix and at 776.0 cm^{-1} in an Ar matrix separately.[6,9] The large shift (139 cm^{-1}) in frequency from argon to neon is unlikely to be due to typical polarizability-based matrix effects, which tend to cause shifts on the order of 5 cm^{-1}–20 cm^{-1} in vibrational frequencies.[35] Jun *et al.*[30] provided the direct evidence of a significant U–Ar bonding interaction when UO_2 is in an argon matrix, showing that this interaction is strong enough to cause the states to have an observable shift. It has been found that even the data for molecules isolated in cryogenic rare gas matrixes, a medium usually considered to be minimally perturbed, can be influenced by the host to a degree that the relationship between the matrix data and the calculations for free molecules is seriously complicated.[5] Hence, our studies should be more suited to describe the vibrational frequencies of an isolated UO_2 molecule.

The vibrational frequencies of UO_3 are also indicated in Table 10. It is clear that our results are in reasonable agreement with experimental values. The maximal IR peak of the ground state structure of the UO_3 molecule is at 880 cm^{-1} with an infrared intensity of 369.03 km/mole, and the corresponding vibrational mode is oxygen stretching vibration.

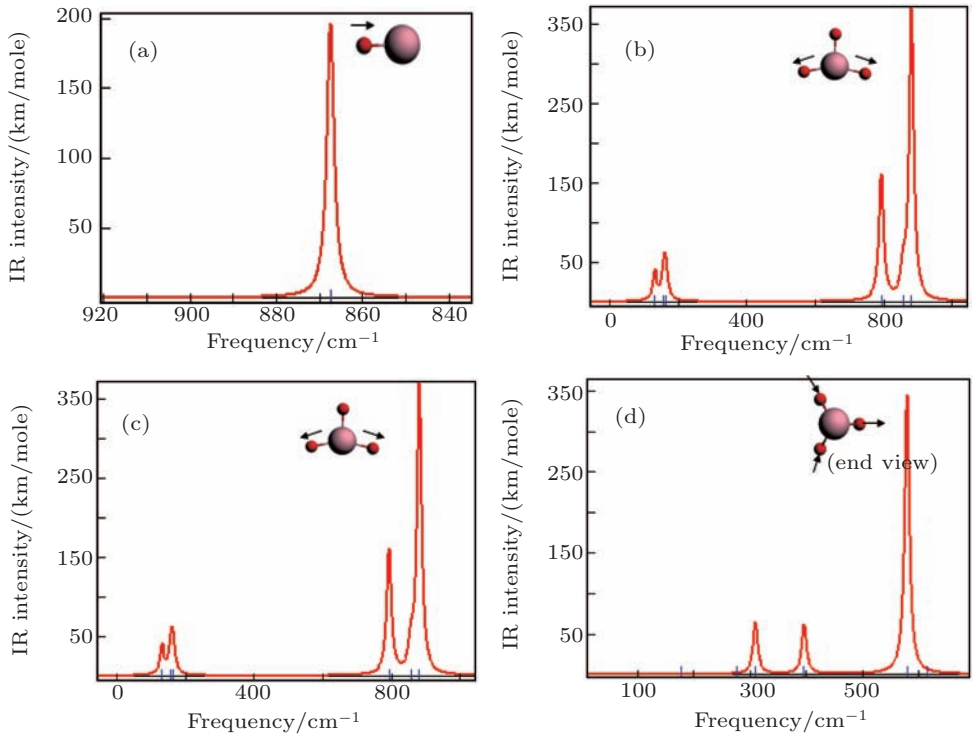


Fig. 4. (colour online) Vibrational spectra and the vibrational modes corresponding to the maximal IR peaks of the ground states of UO, UO_2, UO_3, and U_2O_3 molecules, where panel (a) shows the infrared vibrational spectra of UO, panel (b) the infrared vibrational spectra of UO_2, panel (c) the infrared vibrational spectra of UO_3, and panel (d) the infrared vibrational spectra of U_2O_3.

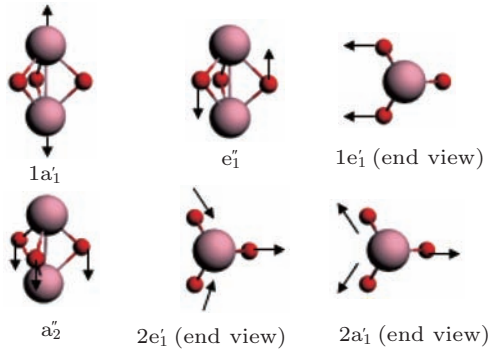


Fig. 5. (colour online) Vibrational modes for the ground state of the U_2O_3 molecule.

Our calculations on the vibrational frequencies of ground state for the U_2O_3 molecule reveal that there are 6 degenerate vibrations in 9 vibrational degrees of freedom, corresponding to computed frequencies of 276.79 (E''_1), 310.77 (E'_1), and 579.15 (E'_1) cm^{-1}. The remaining three nondegenerate frequencies are 178.46 (A'_1), 396.63 (A''_2), and 614.98 (A'_1) cm^{-1}. As shown in Fig. 4(d), the maximal IR peak is at 579 cm^{-1} with an infrared intensity of 353.36 km/mole, which corresponds to oxygen stretching vibration too. Figure 5 shows that the uranium atom has a low frequency component, while the oxygen atom has a high one. It is clear from the computed vibrational frequencies that the method gives a satisfactory description of the equilibrium geometry.

4. Conclusions

The stable structures of UO, UO_2, UO_3, and U_2O_3 molecules are systematically investigated by DFT–GGA calculations. The results show that the bond lengths and harmonic vibration frequencies of the ground states of UO, UO_2, and UO_3 molecules are all in agreement with available experimental data. In geometry optimization of U_2O_3, we test several most possible initial structures with different spin multiplicities (1, 3, 5, 7, 9, 11, 13, and 15). Our calculations indicate that the ground state of the U_2O_3 molecule is $\tilde{X}^7A'_1$ state as a trigonal bipyramid with D_{3h} symmetry (R_1(U–O)=0.2113 nm, R_2(U_1–U_2)=0.2921 nm, $\angle U_1OU_2$=87.5°, dihedral angle Θ(U, O_1, O_2, O_3)=62.40°).

The charge population properties, spin densities and bond orders of UO, UO_2, UO_3, and U_2O_3 molecules are discussed. The results demonstrate that there appears in these molecules the charge transfer from the uranium atom to the oxygen atom, and there are hybrid orbitals mixing the 5f, 6d and 7s orbitals of uranium with the 2p orbital of oxygen. The spin

densities indicate that uranium atoms make positive contributions to the total spin multiplicities for UO, UO_2, and U_2O_3 molecules, while oxygen molecules always contribute to the negative spin. For the UO_3 molecule, the ground state is of holosymmetry, so the spin density of UO_3 ground state is zero. The results of Gophinatan–Jug bond order show that UO, UO_2, and UO_3 molecules possess U=O double bonds properties; U_2O_3 molecule possess U–O single bonds and U–U single bond character.

The frequencies for UO, UO_2, and UO_3 are in good agreement with available experimental data. Our results suggest that there are 6 degenerate vibrations in 9 vibrational degrees of freedom for the ground state of the U_2O_3 molecule, whose frequencies are computed to be 276.79 (E_1''), 310.77 (E_1'), and 579.15 (E_1') cm^{-1}. The remaining three nondegenerated frequencies are 178.46 (A_1'), 396.63 (A_2''), and 614.98 (A_1') cm^{-1}. The maximal IR peak is at 579 cm^{-1} with an infrared intensity of 353.36 km/mole, which corresponds to oxygen stretching.

References

[1] Korzhavyl P A, Leventevitos, Andersson D A and Johansson B 2004 *Nat. Mater.* **3** 225

[2] Guido M and Balducci G 1991 *J. Chem. Phys.* **95** 5373

[3] Lue C J, Jin J, Ortiz M J, Rienstra-Kiracofe J C and Heaven M C 2004 *J. Am. Chem. Soc.* **126** 1812

[4] Infante I, Eliav E, Vilkas M J, Ishikawa Y, Kaldor U and Visscher L 2007 *J. Chem. Phys.* **127** 124308

[5] Gagliardi L, Heaven M C, Krogh J W and Roos B O 2005 *J. Am. Chem. Soc.* **127** 86

[6] Zhou M, Andrews L, Ismail N and Marsden C 2000 *J. Phys. Chem.* A **104** 5495

[7] Zhou M, Andrews L, Li J and Bursten B E 1999 *J. Am. Chem. Soc.* **121** 9712

[8] Tauge J T, Andrews L and Hunt R D 1993 *J. Phys. Chem.* **97** 10920

[9] Hunt R D and Andrews L 1993 *J. Chem. Phys.* **98** 3690

[10] Gagliardi L and Roos B O 2000 *Chem. Phys. Lett.* **331** 229

[11] Gagliardi L, Roos B O, Malmqvis P Å and Dyke J M 2001 *J. Phys Chem.* A **105** 10602

[12] Pyykkö P, Li J and Runeberg N 1994 *J. Phys. Chem.* **98** 4809

[13] Lenthe E V, Baerends E J and Snijders J G 1993 *J. Chem. Phys.* **99** 4597

[14] Lenthe E V, Baerends E J and Snijders J G 1994 *J. Chem. Phys.* **101** 9783

[15] Lenthe E V, Baerends E J and Snijders J G 1999 *J. Chem. Phys.* **110** 8943

[16] Perdew J P 1986 *Phys. Rev.* B **33** 8822

[17] Perdew J P 1986 *Phys. Rev.* B **34** 7406

[18] Perdew J P and Wang Y 1992 *Phys. Rev.* B **45** 13244

[19] Becke A D 1986 *J. Chem. Phys.* **84** 4524

[20] Becke A D 1993 *J. Chem. Phys.* **98** 5648

[21] Shannon R D 1976 *Acta Crys. Sect.* A **32** 751

[22] Lyon J T, Hu H S, Andrews L and Li J 2007 *PNAS* **104** 18919

[23] Zhang Y G and Li Y D 2010 *Chin. Phys.* B **19** 033302

[24] Moskaleva L V, Matveev A V, Krüger S and Rösch N 2006 *Chem. Eur. J.* **12** 629

[25] Moskaleva L V, Matveev A V, Dengler J and Rösch N 2006 *Phys. Chem. Chem. Phys.* **8** 3767

[26] Chen J, Meng D Q, Du J G, Jiang G, Gao T and Zhu Z H 2010 *Acta Phys. Sin.* **59** 1658 (in Chinese)

[27] Lenthee E V, Bearends E J and Snijders J G 1994 *J. Chem. Phys.* **101** 9783

[28] Lenthee E V, Snijders J G and Bearends E J 1996 *J. Chem. Phys.* **105** 6505

[29] Kaledin L A and Heaven M C 1997 *J. Mol. Spectr.* **185** 1

[30] Jun L, Bursten B E, Andrews L and Marsden C J 2004 *J. Am. Chem. Soc.* **126** 3424

[31] Herzberg G 1966 *Molecular Spectra and Molecular Structure* III (New York: Van Nostrand Reinhold Company) pp. 570–572

[32] Ruiz-Morales Y 2002 *J. Phys. Chem.* A **106** 11283

[33] Xu G X and Wang X Y 2010 *The Structure of Matter* (Beijing: Science Press) pp. 72, 94 (in Chinese)

[34] Green D W, Reedy G T and Gabelnick S D 1980 *J. Chem. Phys.* **73** 4207

[35] Jacox M E 1994 *Chem. Phys.* **189** 149